Proc. Natl. Acad. Sci. USA
Vol. 91, pp. 2095–2099, March 1994
Cell Biology

Molecular analysis of cell surface β-1,4-galactosyltransferase function during cell migration

PAUL A. APPEDDU AND BARRY D. SHUR*

Department of Biochemistry and Molecular Biology, Box 117, The University of Texas M. D. Anderson Cancer Center, 1515 Holcombe Boulevard, Houston, TX 77030

Communicated by George M. Whitesides, October 18, 1993

ABSTRACT **Despite the identification and characterization of cell surface receptors for the extracellular matrix, it is unknown how their relative expression and cytoskeletal association regulate cell migration. Previous studies have identified β-1,4-galactosyltransferase (GalTase; EC 2.4.1.38) on the surface of migrating cells, where it mediates cell migration on basal lamina matrices by associating with the cytoskeleton and binding to N-linked oligosaccharides in the E8 domain of laminin. In this study, the function of GalTase during cell migration was examined directly by analyzing the migration rate of stably transfected cell lines in which the relative level of surface GalTase and its ability to associate with the cytoskeleton were altered. We show here that the cytoskeleton contains a limiting, saturable, number of binding sites for surface GalTase. Furthermore, the rate of cell migration was inversely related to the ability of surface GalTase to associate with the cytoskeleton. Elevating surface GalTase in excess of the number of cytoskeleton-binding sites reduced the rate of cell migration, whereas decreasing the amount of surface GalTase available to bind the cytoskeleton increased migration rates. These results show that the rate of cell migration on basal lamina is directly dependent upon the expression of surface GalTase and the ability of this protein to associate with a limiting number of cytoskeleton-binding sites.**

Cell migration is crucial to such diverse processes as embryonic morphogenesis and metastatic invasion and requires the concerted action of many intracellular, plasma membrane, and extracellular components (for review, see refs. 1–5). One previously identified laminin receptor that functions during the migration of several cell types is β-1,4-galactosyltransferase (GalTase; EC 2.4.1.38). GalTase is unusual in that it resides in two distinct subcellular locations, where it performs different functions (6). Most GalTase is localized in the trans-Golgi complex, where it participates in glycoprotein biosynthesis. A subpopulation of GalTase is also present on the cell surface, where it functions as a cell adhesion molecule by binding to specific oligosaccharide ligands on adjacent cell surfaces and in the extracellular matrix. Recent evidence suggests that GalTase functions as a cell adhesion molecule by virtue of a 13 amino acid cytoplasmic sequence that targets a portion of this protein from the Golgi complex to the cell surface (7).

On the cell surface, GalTase mediates several types of cellular interactions with the basal lamina by binding to N-linked oligosaccharides present in the E8 domain of laminin (8). Furthermore, the biological activity of E8 can be shown to be at least partly dependent upon binding to surface GalTase, since biological activity is lost when GalTase-binding sites of E8 are masked by prior galactosylation or removed by glycosidase digestion (8). Examples of GalTase-dependent cell interactions with laminin include the migration of quail and chick neural crest cells, mouse embryonic fibroblasts, and melanoma cells and neurite outgrowth from PC12 cells and dorsal root ganglia (for review, see ref. 6). By indirect immunofluorescence, GalTase is found at the leading edge of migrating cells (9) and at the tips of extending neurites (10), where it participates in lamellipodial and axonal formation. Furthermore, surface GalTase is associated with the detergent-insoluble cytoskeleton (11), which is required for GalTase to function as a cell adhesion molecule; GalTase that is not associated with the cytoskeleton can still bind its glycoside substrates, but it is unable to mediate cell adhesion and spreading on laminin matrices (12). The precise mechanism by which GalTase associates with the cytoskeleton remains obscure, but preliminary evidence suggests the involvement of an 80- to 85-kDa phosphoprotein (D. H. Dubois and B.D.S., unpublished data).

Although it is known that the localization (13) as well as the function (12, 14) of some cell adhesion molecules, including GalTase, can be affected by their association with the cytoskeleton, our knowledge of the interrelationship of these molecules during cell migration is lacking. For instance, it is still unknown how cell migration is regulated by the relative abundance of cell surface matrix receptors and their cytoskeleton-binding sites. Increasing the quantity of matrix receptors able to bind the cytoskeleton could conceivably facilitate lamellipodial formation and increase cell migration rate; alternatively, decreasing the number of receptor–cytoskeleton complexes may allow cells to move more rapidly. We have addressed these possibilities by analyzing the migratory rate of cell lines that express either increased or decreased levels of surface GalTase relative to its cytoskeleton-binding sites. We report here that the rate of cell migration on basal lamina matrices is directly dependent upon surface GalTase expression and is inversely proportional to the ability of surface GalTase to interact with the cytoskeleton.

MATERIALS AND METHODS

Cell Culture and Transfection. Mouse embryo Swiss 3T3 fibroblasts were cultured and stably transfected as previously described (7, 12); 50×10^5 cells were transfected with 2 μg of pKJ-*neo* and 20 μg of either promoter-deleted long GalTase (PDLGT; nt −9 to 1265) (7) or truncated long GalTase (TLGT; nt −9 to 142) (12) cDNA. Stable G418-resistant (*neo*-containing) clones were isolated and expanded.

S1 Nuclease Protection Analysis. S1 nuclease protection analyses were performed as described previously, using ^{32}P-labeled DNA probes complementary to transcribed sequences (7, 12). After hybridization overnight at 59°C, followed by S1 nuclease digestion for 1.5 hr at 37°C, the

The publication costs of this article were defrayed in part by page charge payment. This article must therefore be hereby marked "*advertisement*" in accordance with 18 U.S.C. §1734 solely to indicate this fact.

Abbreviations: GalTase, β-1,4-galactosyltransferase; PDLGT, promoter-deleted long GalTase; TLGT, truncated long GalTase.
*To whom reprint requests should be addressed.

protected fragments were analyzed on an 8 M urea/6% polyacrylamide gel.

Cell Surface GalTase Activity. Cell surface GalTase activity toward *N*-acetylglucosamine substrates was assayed as described (12). Cells ($3–5 \times 10^5$; >95% viability) were incubated in medium B with 100 μM UDP[^{3}H]Gal (17.6 cpm/pmol) (DuPont/NEN), 30 mM *N*-acetylglucosamine, 10 mM $MnCl_2$, 1 mM 5′-AMP, 0.4% bovine serum albumin, and protease inhibitor cocktail (12). Samples (50 μl) were removed at the indicated times and subjected to high-voltage borate electrophoresis to separate the ^{3}H-labeled galactosylated product from unused UDP[^{3}H]Gal and its breakdown products.

GalTase Association with the Cytoskeleton. The association of surface GalTase with the Triton-insoluble cytoskeleton was assayed as described (11). Intact viable cells were incubated with rabbit anti-GalTase IgG, washed, incubated with ^{125}I-labeled goat anti-rabbit IgG, washed, and extracted three times with Triton X-100 to remove all soluble radioactivity. Anti-GalTase specific immunoreactivity remaining in the detergent-insoluble cytoskeleton pellet was determined by subtracting the cpm associated with preimmune rabbit controls. The concentrations of both the primary and the ^{125}I-labeled secondary antibodies were shown to be in excess. The anti-GalTase IgG specifically recognizes GalTase on mouse cells as judged by immunoprecipitation and immunoblotting criteria (11, 15–17).

Wounding Migration Assay. Cell monolayers were cultured to confluence on laminin-coated 35-mm dishes and washed with Ca- and Mg-free Eagle's balanced salt solution (CMF-BSS). Cell migration was initiated by "wounding" the confluent monolayer with a cell scraper. The monolayers were washed with CMF-BSS, and 2 ml of growth medium was added. Cell migration was quantified by using photographs taken at 2-hr intervals after the addition of growth medium. The mean distance from a defined line in the middle of the wound to the nuclei of the 20 furthest-migrating cells in a particular frame was measured by using a Kurta digitizing board (Kurta, Phoenix, AZ) and SigmaScan software (Jandel, Corte Madera, CA) and then normalized to a standard field width. Distance migrated was calculated from the mean distances in successive frames of a particular field. To fully induce the metallothionein promoter, 80 μM $ZnSO_4$ (final concentration) was added to TLGT cells 6 hr before the monolayer was wounded. During the migration assay also, the medium contained 80 μM $ZnSO_4$.

Cell Size Analysis. Cells plated on laminin-coated dishes were photographed and then dissociated with 2 mM EDTA. After being washed in Dulbecco's modified Eagle's medium, an aliquot of the cells was placed on a hemacytometer and photographed. Cell areas were calculated from perimeters of plated cells digitized and analyzed by using SigmaScan, whereas cell volume in suspension was calculated from the cross-sectional area of cells.

RESULTS AND DISCUSSION

Production of Stable Cell Lines with Increased or Decreased Surface GalTase. We wished to determine how altering the quantity of surface GalTase affected its ability to interact with the cytoskeleton and how this would affect the rate of cell migration. Stably transfected cell lines were created that exhibited either increased or decreased levels of surface GalTase capable of interacting with the cytoskeleton. Cell lines with increased surface GalTase were created by transfecting murine Swiss 3T3 fibroblasts with a neomycin-selectable marker (pKJ-*neo*) and the pKJ-PDLGT vector (7). The pKJ-PDLGT vector contains cDNA encoding the full-length long form of GalTase under control of the constitutive phosphoglycerokinase promoter (Fig. 1). After selection for

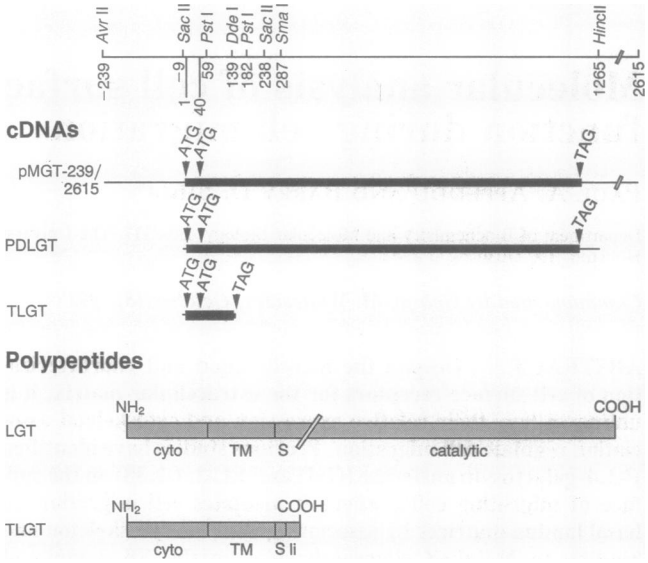

FIG. 1. PDLGT and TLGT cDNA clones and polypeptides. The promoter-deleted long GalTase (PDLGT; nt −9 to 1265) cDNA was derived from pMGT-239/2615 as previously described (7), and encodes primarily the long GalTase protein (7, 12). The truncated long GalTase (TLGT; nt −9 to 142) cDNA was obtained from PDLGT (12). The PDLGT construct was inserted into the pKJ-*neo* expression vector under the control of the phosphoglycerokinase promoter. The TLGT construct was inserted into the *Bgl* II site of the EV-142 expression vector under the control of the metallothionein 1 promoter. Whereas both full-length long GalTase (LGT) and TLGT proteins have identical N-terminal cytoplasmic (cyto) and transmembrane (TM) domains, the TLGT protein lacks the extracellular catalytic domain (catalytic); only three amino acids of the stem (S) region remain. The C terminus of the TLGT contains four amino acids derived from *Xba* I linkers (li). These plasmids were cotransfected with a neomycin-selectable marker into Swiss 3T3 cells.

G418 resistance, expression of the exogenous mRNA was verified by S1 nuclease protection analysis, and surface GalTase expression was quantified by enzymatic assay. In each of three independent pKJ-PDLGT-transfected clones chosen for further analysis (D6, D16, and D31), a 296-nt RNA species was protected, corresponding to an mRNA coding for the full-length long GalTase protein (7) (Fig. 2). This transcript is distinct from the endogenous GalTase transcripts due to deletion of 5′ untranslated sequences in the pKJ-PDLGT construct (7); it was not expressed in the parental 3T3 cell line or in two control clones transfected with pKJ-*neo* only (A5 and N6) (Fig. 2). Consistent with overexpression of the long-form mRNA, surface GalTase activities of the three PDLGT cell lines averaged ≈8 times the activity of controls (Table 1).

Cell lines with decreased levels of surface GalTase capable of interacting with the cytoskeleton have been recently described (12). In this case, 3T3 fibroblasts were transfected with cDNAs encoding a truncated, catalytically inactive GalTase protein corresponding to the complete cytoplasmic and transmembrane domains of the long form of GalTase under the control of the metallothionein promoter (Fig. 1). The truncated GalTase (TLGT) protein produces a dominant negative mutation in surface GalTase function by specifically displacing the endogenous full-length GalTase from its cytoskeletal association. Although the full complement of surface GalTase remains present in the plasma membrane, it is no longer able to function as a laminin receptor due to its displacement from the cytoskeleton (12). Two independent TLGT clones were used in the present analysis, TL61 and TL64. In those cell types thus far examined, expression of either the TLGT or the PDLGT proteins has no apparent

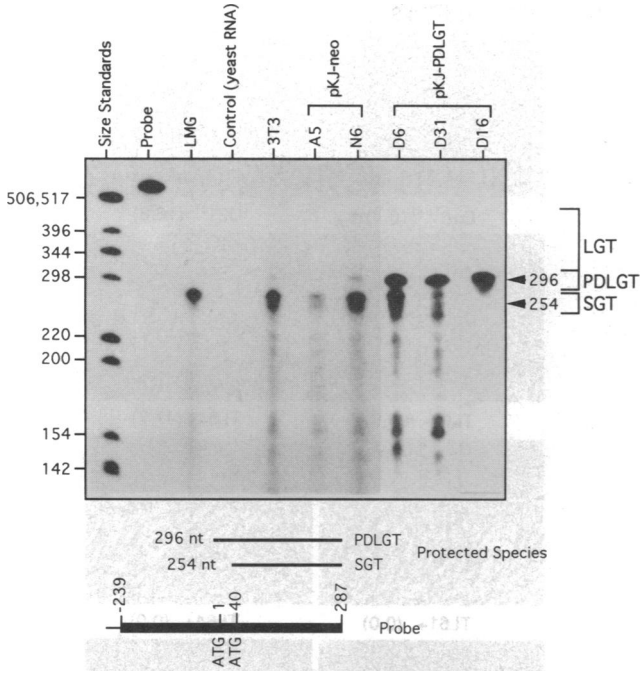

FIG. 2. S1 nuclease protection analysis of GalTase RNA expression in PDLGT clones. Samples (10 μg) of partially hydrolyzed yeast RNA, total cellular RNA from 3T3 fibroblasts, two independent control pKJ-*neo* 3T3 cell transfectants (A5 and N6), three independent pKJ-PDLGT 3T3 cell transfectants (D6, D16, and D31), and lactating mammary gland (LMG) were analyzed by S1 nuclease protection analysis (7, 12). The 567-nt probe, which was derived from clone pMGT-239/2615 (7), contains 239 nt of GalTase 5′-untranslated sequence, 290 nt of translated sequence (3 nt derived from linker) (thick line), and 38 nt of vector sequences (thin line). Arrowheads to the right represent the sizes of the major protected species, and the regions corresponding to long GalTase (LGT), PDLGT, and short GalTase (SGT) transcripts are indicated. Undigested radiolabeled DNA probe was also analyzed on the gel. Molecular size markers (nt) are 1-kb DNA ladder. The lactating mammary gland produces almost exclusively short GalTase transcripts, which are also seen in the various 3T3 cell lines. All lanes are from the same gel, except D16. The three PDLGT lanes are shown at a lighter exposure than the other lanes, due to the high levels of PDLGT transgene expression. At these exposures, transcripts corresponding to the endogenous long GalTase are undetectable.

effect on endogenous glycoprotein biosynthesis or overall cellular metabolism (12, 18).

The Cytoskeleton Has a Limited Number of Binding Sites for GalTase. Because GalTase is associated with the cytoskeleton (11, 12), we determined whether the increased expression of surface GalTase in PDLGT clones led to a subsequent increase in the amount of GalTase associated with the cytoskeleton. Despite the 8-fold increase in surface GalTase expression, there was no significant increase in the amount of GalTase associated with the cytoskeleton (Table 1). Therefore, the amount of GalTase capable of interacting with the cytoskeleton was in vast excess to the number of cytoskeleton-binding sites. In contrast, only about half of the surface GalTase is able to bind the cytoskeleton in TLGT cells because the full-length surface GalTase is displaced from the cytoskeleton by an approximately equimolar concentration of the TLGT protein expressed under standard culture conditions (12). Further increases in TLGT protein expression brought about by inducing the metallothionein promoter result in a concomitant loss in surface GalTase association with the cytoskeleton (12). Thus, these results support the hypothesis that the cytoskeleton has a defined, saturable number of binding sites for GalTase. These sites are at least partly specific for GalTase, since expression of the TLGT protein fails to affect the cytoskeleton association of another matrix receptor, β1 integrin (12).

Table 1. Surface GalTase activity and association with the Triton-insoluble cytoskeleton

Cell type	Surface GalTase	
	Activity on intact cells	Associated with cytoskeleton
Control (3)	1.00 ± 0.12	1.00 ± 0.21
PDLGT (3)	7.77 ± 4.76*	1.28 ± 0.33
TLGT (2)	0.98 ± 0.11	0.59 ± 0.03*

Cell surface GalTase activity toward *N*-acetylglucosamine substrates was assayed as a function of time (12). Assays were performed in duplicate, and at least three determinations were made for each cell line. The numbers in parentheses represent the number of independent clones analyzed. All results are presented relative to control and are mean ± SEM. The association of surface GalTase with the Triton X-100-insoluble cytoskeleton was assayed by binding anti-GalTase IgG to intact viable cells and quantifying the IgG partitioning with the detergent-insoluble cytoskeleton, using radiolabeled secondary antibodies (11). Assays were performed in duplicate, and at least six determinations were made for each cell line. Data for TLGT cells are from ref. 12.
*$P < 0.05$ relative to control.

Cell Migration Rate Is Inversely Related to the Amount of GalTase Associated with the Cytoskeleton. Having created cell lines with either increased or decreased levels of GalTase available to bind the cytoskeleton, we examined the migration of these cells after their release from contact inhibition. Photographs were taken at 2-hr intervals after wounding a dish of confluent cells and used to determine the rate of cell migration into the cell-free space. Due to contact with neighboring cells during the assay, cells migrate into the wound in a nearly unidirectional manner. Surprisingly, PDLGT cells, which express increased levels of surface GalTase that would be expected to facilitate cell interactions with laminin and increase migration rate, migrated at only half the rate of control cells (13.1 ± 2.5 vs. 26.5 ± 3.4 μm/hr). In contrast, TLGT cells, in which surface GalTase has a limited ability to bind the cytoskeleton, migrated at more than twice the rate of control cells (57.9 ± 6.3 μm/hr) (Fig. 3). Under extreme conditions, when the TLGT protein was grossly overexpressed by inducing the metallothionein promoter, most of the cytoskeleton-binding sites were occupied

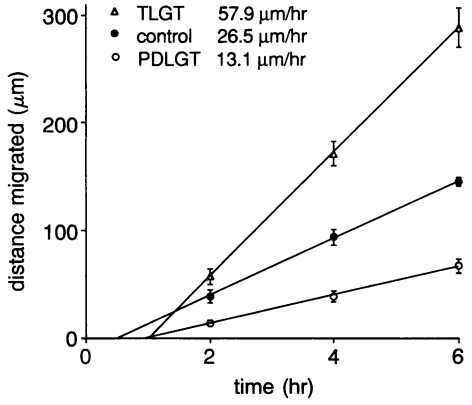

FIG. 3. The rate of cell migration is dictated by the level of surface GalTase associated with the cytoskeleton. Cell migration was initiated by wounding a confluent monolayer with a cell scraper 2 days after plating cells on laminin-coated 35-mm dishes. The graphs represent the average distance migrated ± SEM of two independent cell lines of each type. PDLGT cells, in which surface GalTase is in vast excess to the number of cytoskeleton-binding sites, migrated at approximately half the rate of control cells, whereas TLGT cells, in which about half of the cytoskeleton-binding sites are occupied by truncated GalTase protein, migrated twice as fast as controls.

with TLGT protein and unavailable to bind GalTase (12), which precluded lamellipodia formation and subsequent migration (see Fig. 5; TL61+, TL64+). In separate assays, the behavior of PDLGT and TLGT clones was indistinguishable from control cells when plated on fibronectin, which was expected since cell interactions with fibronectin are GalTase independent (ref. 12 and unpublished results). Collectively, these results suggest that cell migration is inversely proportional to the amount of surface GalTase associated with the cytoskeleton, as long as a threshold amount of GalTase is bound to the cytoskeleton, enabling lamellipodia formation.

Analysis of the migratory behavior of the individual PDLGT and TLGT clones well illustrates the dependency of cell migration on the ability of GalTase to associate with the cytoskeleton (Fig. 4). Cells (D16) with the highest surface GalTase expression (17.2 times control), and therefore the highest GalTase-to-cytoskeleton ratio, migrated the slowest of all cell lines (10.4 μm/hr), whereas cells (D31) with moderate increases in surface GalTase expression (2.2 times control), and therefore more normal GalTase-to-cytoskeleton ratios, migrated closer to normal rates (16.8 μm/hr; controls: 26.5 μm/hr). Similarly, cells (TL61) with only 46% of their surface GalTase associated with the cytoskeleton migrated more rapidly (65.6 μm/hr) than did cells (TL64) in which 65% of their surface GalTase was cytoskeletally associated (47.7 μm/hr). However, the relationship between migration rate and the ratio of surface GalTase to its cytoskeleton-binding sites was not linear. Small increases in surface GalTase dramatically affected cell migration rate until GalTase levels reached approximately twice the level of control cells, at which point cytoskeleton availability appears to have been so rate-limiting that further increases in GalTase expression had less dramatic effects on migratory rate (Fig. 4).

Differences in migration rates were not the result of differences in cell spreading or lamellipodia size. All cell types were able to spread equally well, as assayed by the ratio of their spread surface area to volume (determined as described in *Materials and Methods*): controls, 0.234 ± 0.063 surface area/volume; PDLGT, 0.282 ± 0.056; TLGT, 0.281 ± 0.008. Furthermore, N6 and 3T3 control cells had similar migration rates, even though N6 cells had characteristically larger lamellipodia (Fig. 5). Likewise, migration rates were similar between D16 and D31 PDLGT clones despite their different lamellipodia sizes. The characteristically different migration rates of cells with similar lamellipodia sizes (i.e., 3T3 and D16, N6 and D31) could be attributed only to the level of surface GalTase available to bind the cytoskeleton.

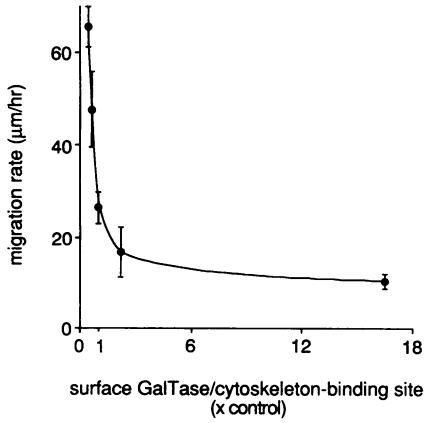

FIG. 4. The relationship between migration rate and the ratio of surface GalTase to its cytoskeleton-binding sites is not linear. The migratory rate characteristic of each clone (±SEM) is plotted relative to the amount of surface GalTase available to bind the cytoskeleton. Migration rate is very sensitive to small differences in GalTase levels available to bind the cytoskeleton, but once surface GalTase levels reach approximately twice control levels, cytoskeleton availability becomes so rate-limiting that additional increases in GalTase have less significant effects on migration rate.

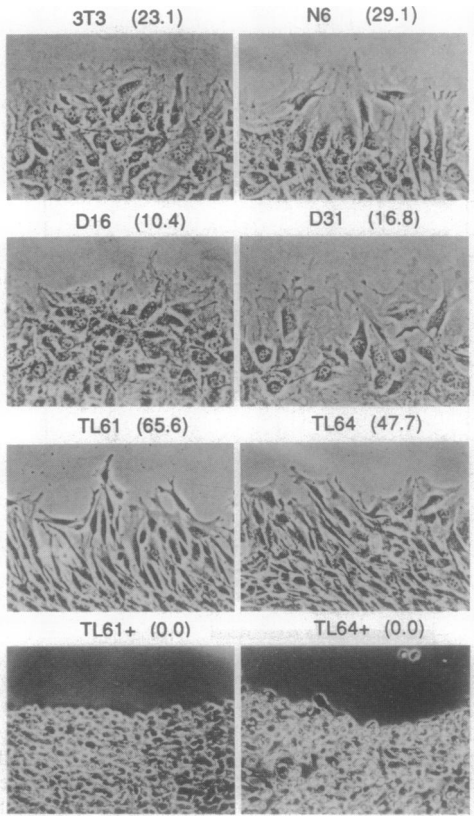

FIG. 5. Lamellipodia size is unrelated to migration rate or surface GalTase activity. The leading edges of confluent monolayers are shown 4–6 hr after wounding along with, in parentheses, migration rate in μm/hr. Lamellipodia size was relatively consistent within each clonal population. Cells with similar lamellipodia sizes (i.e., 3T3 and D16, N6 and D31) had characteristically different migration rates that could be attributed only to the level of surface GalTase available to bind the cytoskeleton. Overexpressing TLGT protein production by inducing the metallothionein promoter displaces most surface GalTase from the cytoskeleton and precludes lamellipodia formation and cell migration. Cells: 3T3 and N6, controls; D16 and D31, PDLGT; TL61 and TL64, TLGT; and TL61+ and TL64+, TLGT-induced.

Although the results show clearly that cell migration rate is inversely related to the ability of surface GalTase to bind the cytoskeleton, the underlying mechanisms are less clear. In one possible scenario, diagrammed in Fig. 6, the rate of cell migration may be dictated by the relative translocation of the GalTase–laminin adhesive complex at the leading edge of the cell. In this model, new cytoskeletal associations are formed with GalTase at what will become the leading edge of the cell, coincident with disassembly of preexisting cytoskeleton–GalTase complexes. The increased expression of GalTase in PDLGT cells may decrease migration rate by increasing the density of GalTase presented to the cytoskeleton, thus reducing the distance between successive adhesion complexes. In contrast, TLGT (truncated) proteins hinder the efforts of the cytoskeleton to locate and bind endogenous full-length GalTase, in effect diluting the density of functional GalTase–cytoskeleton complexes. The effective decrease in the number of cytoskeleton–GalTase–laminin complexes may allow for rapid cell body displacement that is not possible in control or PDLGT cells.

Alternatively, the migration rate of these transfectants might reflect changes in the avidity, or strength, of the

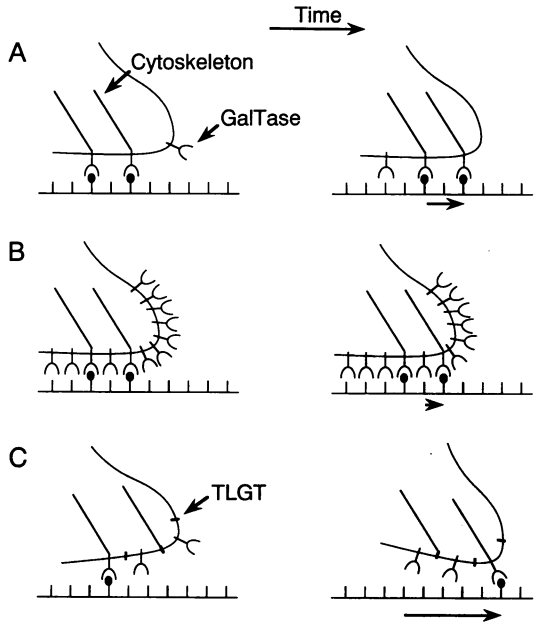

FIG. 6. Cell migration is inversely proportional to the amount of surface GalTase available to bind the cytoskeleton. In this hypothetical model, migration occurs by the formation of new cytoskeleton–GalTase–laminin complexes (denoted by the black balls) at the leading edge of the cell. Previous studies have shown that only cytoskeletally bound GalTase is able to function as a cell adhesion molecule (12). (*A*) In control cells, most surface GalTase is found associated with the cytoskeleton (11). As the leading edge of the cell advances, the cytoskeleton associates with the next available cytoplasmic tail of GalTase, thus shifting forward the adhesive complex by the distance denoted by the horizontal arrow. (*B*) Due to the increased density of surface GalTase in PDLGT cells, the relative distance between cytoskeletally associated adhesion complexes may be reduced. In this case, the newly formed adhesion at the leading edge has advanced only half the distance of that in control cells, thus reducing migration rate by half. Alternatively, increasing surface GalTase expression in PDLGT cells may increase the avidity of the adhesion complex, thereby reducing migration rate. (*C*) Expression of an approximately equimolar concentration of TLGT (truncated) protein in TLGT cells reduces by half the ability of the cytoskeleton to bind a full-length GalTase molecule capable of forming a functional adhesion complex with matrix oligosaccharides. Thus, the leading edge advances at twice the rate of control cells.

surface GalTase–laminin adhesion complex. In general, cell surface lectinlike molecules have low affinity for their glycoside ligands, which is thought to facilitate transient binding with the extracellular matrix during carbohydrate-dependent cell interactions, such as lymphocyte "rolling" (19) and cell migration (8–10). Increasing the ability of GalTase to associate with the cytoskeleton in PDLGT cells may increase the strength, or avidity, of the cell–matrix adhesion complex, thus reducing migration rate. Decreasing the propensity of GalTase to associate with the cytoskeleton in TLGT cells could lead to a decreased adhesive avidity, accelerating migration rate. Studies by others have, in fact, suggested that the rate of cell migration on fibronectin matrices is directly related to the avidity of the integrin–matrix complex (20).

In a similar manner, the increased density of GalTase in PDLGT cells may permit clustering of GalTase by laminin, which could lead to nucleation of cytoskeletal stress fibers that would oppose cell migration (21, 22), whereas TLGT cells may be unable to achieve a sufficient density of cytoskeletally associated GalTase to initiate stress fiber formation. Regardless of the underlying mechanisms, there appears to be a threshold level of cytoskeleton–GalTase–laminin complexes necessary for cell migration, since cells nearly completely deficient in cytoskeletally associated GalTase do not form lamellipodia and do not migrate (see Figs. 3 and 5).

To date, all studies of surface GalTase function during cell migration have been limited to the use of exogenous reagents that block GalTase activity, such as competitive substrates and antibodies. However, the recent cloning of GalTase cDNAs encoding the surface and Golgi proteins has allowed a more direct analysis of surface GalTase function by altering its relative level of expression (7, 12). We show here that altering the level of surface GalTase directly affects cell migration rate. However, it is surprising that drastic changes in the amount of surface GalTase available to bind the cytoskeleton led to subsequent changes in migration rate without affecting the size of lamellipodia, the principal migratory apparatus of the cell (23). Furthermore, the rate of cell migration was independent of the absolute concentration of surface GalTase, since control and TLGT cells had similar GalTase levels but different migration rates. Nor were differences in cell migration the result of differences in the level of GalTase-binding sites in the cytoskeleton, which remained constant in all cell types, or differences in matrix concentration, which was not manipulated in this study. Rather, the rate of cell migration was the direct consequence of the relative amount of surface GalTase available to bind the cytoskeleton; increasing GalTase levels decreased migration rate, whereas decreasing GalTase levels increased migration. This suggests that cells may regulate their migration by altering the relative quantities of either specific matrix receptors or their cytoskeleton-associated proteins.

This work was supported by Grant DE 07120 from the National Institutes of Health to B.D.S. and by Institutional National Institutes of Health Predoctoral Training Grant HD 07325 to P.A.A.

1. Hay, E. D. (1990) *Cell Differ. Dev.* **32,** 367–375.
2. Akiyama, S. K., Nagata, K. & Yamada, K. M. (1990) *Biochim. Biophys. Acta* **1031,** 91–110.
3. Mecham, R. P. (1991) *FASEB J.* **5,** 2538–2546.
4. Hynes, R. O. (1992) *Cell* **69,** 11–25.
5. Luna, E. J. & Hitt, A. L. (1992) *Science* **258,** 955–964.
6. Shur, B. D. (1993) *Curr. Opin. Cell Biol.* **5,** 854–863.
7. Lopez, L. C., Youakim, A., Evans, S. C. & Shur, B. D. (1991) *J. Biol. Chem.* **266,** 15894–15991.
8. Begovac, P. C., Hall, D. E. & Shur, B. D. (1991) *J. Cell Biol.* **113,** 637–644.
9. Eckstein, D. J. & Shur, B. D. (1989) *J. Cell Biol.* **108,** 2507–2517.
10. Begovac, P. C. & Shur, B. D. (1990) *J. Cell Biol.* **110,** 461–470.
11. Eckstein, D. J. & Shur, B. D. (1992) *Exp. Cell Res.* **201,** 83–90.
12. Evans, S. C., Lopez, L. C. & Shur, B. D. (1993) *J. Cell Biol.* **120,** 1045–1057.
13. Solowska, J., Guan, J.-L., Marcantonio, E. E., Trevithick, J. E., Buck, C. A. & Hynes, R. O. (1989) *J. Cell Biol.* **109,** 853–861.
14. Kintner, C. (1992) *Cell* **69,** 225–236.
15. Macek, M. B., Lopez, L. C. & Shur, B. D. (1991) *Dev. Biol.* **147,** 440–444.
16. Bayna, E. M., Shaper, J. H. & Shur, B. D. (1988) *Cell* **53,** 145–157.
17. Lopez, L. C., Bayna, E. M., Litoff, D., Shaper, N. L., Shaper, J. H. & Shur, B. D. (1985) *J. Cell Biol.* **101,** 1501–1510.
18. Youakim, A. & Shur, B. D. (1993) *Glycobiology* **3,** 155–163.
19. Rosen, S. D. (1989) *Curr. Opin. Cell Biol.* **1,** 913–919.
20. Duband, J.-L., Dufour, S., Yamada, S. S., Yamada, K. M. & Thiery, J. P. (1991) *J. Cell Sci.* **98,** 517–532.
21. Couchman, J. R. & Rees, D. A. (1979) *J. Cell Sci.* **39,** 149–165.
22. Wehland, J., Osborn, M. & Weber, K. (1977) *Proc. Natl. Acad. Sci. USA* **84,** 5613–5617.
23. Abercrombie, M., Heaysman, J. E. M. & Pegrum, S. M. (1970) *Exp. Cell Res.* **59,** 393–398.